CLIMATE CHANGE PROJECTED SANTA ANA FIRE WEATHER OCCURRENCE

DRAFT

A Report From:
California Climate Change Center

Prepared By:
Norman L. Miller, Atmosphere and Ocean Sciences Group, Earth Sciences Division, Lawrence Berkeley National Laboratory

Nicole J. Schlegel, Department of Earth and Planetary Science, University of California, Berkeley

WHITE PAPER

DISCLAIMER

This report was prepared as the result of work sponsored by the California Energy Commission (Energy Commission) and the California Environmental Protection Agency (Cal/EPA). It does not necessarily represent the views of the Energy Commission, Cal/EPA, their employees, or the State of California. The Energy Commission, Cal/EPA, the State of California, their employees, contractors, and subcontractors make no warrant, express or implied, and assume no legal liability for the information in this report; nor does any party represent that the uses of this information will not infringe upon privately owned rights. This report has not been approved or disapproved by the California Energy Commission or Cal/EPA, nor has the California Energy Commission or Cal/EPA passed upon the accuracy or adequacy of the information in this report.

Arnold Schwarzenegger, *Governor*

December 2005
CEC-500-2005-204-SD

Acknowledgements

Support for this study provided by the California Environmental Protection Agency as a contribution to the Climate Change Science Report to the Governor. We thank Katharine Hayhoe of the Department of Geosciences, Texas Technical University and Mary Tyree of the Climate Research Division, Scripps Institution of Oceanography for AOGCM data support. Code development for this work was performed by Nicole J. Schlegel. This report is LBNL-59125.

Preface

The Public Interest Energy Research (PIER) Program supports public interest energy research and development that will help improve the quality of life in California by bringing environmentally safe, affordable, and reliable energy services and products to the marketplace.

The PIER Program, managed by the California Energy Commission (Energy Commission), annually awards up to $62 million to conduct the most promising public interest energy research by partnering with Research, Development, and Demonstration (RD&D) organizations, including individuals, businesses, utilities, and public or private research institutions.

PIER funding efforts are focused on the following RD&D program areas:

- Buildings End-Use Energy Efficiency
- Energy-Related Environmental Research
- Energy Systems Integration
- Environmentally Preferred Advanced Generation
- Industrial/Agricultural/Water End-Use Energy Efficiency
- Renewable Energy Technologies

The California Climate Change Center (CCCC) is sponsored by the PIER program and coordinated by its Energy-Related Environmental Research area. The Center is managed by the California Energy Commission, Scripps Institution of Oceanography at the University of California at San Diego, and the University of California at Berkeley. The Scripps Institution of Oceanography conducts and administers research on climate change detection, analysis, and modeling; and the University of California at Berkeley conducts and administers research on economic analyses and policy issues. The Center also supports the Global Climate Change Grant Program, which offers competitive solicitations for climate research.

The California Climate Change Center Report Series details ongoing Center-sponsored research. As interim project results, these reports receive minimal editing, and the information contained in these reports may change; authors should be contacted for the most recent project results. By providing ready access to this timely research, the Center seeks to inform the public and expand dissemination of climate change information; thereby leveraging collaborative efforts and increasing the benefits of this research to California's citizens, environment, and economy.

For more information on the PIER Program, please visit the Energy Commission's website www.energy.ca.gov/pier/ or contact the Energy Commission at (916) 654-5164.

Table of Contents

Preface ii
1.0 INTRODUCTION 1
2.0 APPROACH 1
3.0 RESULTS 2
4.0 SUMMARY AND CONCLUSION 3
5.0 REFERENCES 4

List of Figures

Figure 1. A four-day snapshot of the time evolving geopotential height fields, constrained by ERA40 specific humidity, associated with the December 1999 Santa Ana fires. 7

Figure 2. GFDL AOGCM derived number of SAO days based on the pressure gradient and humidity indicate a small bias for the monthly climatological occurrences. 8

Figure 3. AOGCM-derived SAO sensitivity for 2005-2034, 2035-2064, and 2070-2099 based (A) GFDL pressure gradients and humidity with A2 forcing, (B) GFDL pressure gradients with A2 forcing, and (C) GFDL pressure gradients B1 forcing. 9

Figure 4. AOGCM-derived SAO sensitivity for 2005-2034, 2035-2064, and 2070-2099 based (A) PCM pressure gradients with A2 forcing, (B) PCM pressure gradients B1 forcing. 10

Figure 5. Comparison of the observed SAOs and southern California sea surface temperatures for September-December during 1965-1994. 11

List of Tables

Table 1. Evaluation of the derived SAO using GFDL A2 constrained and unconstrained by humidity 5

Table 2a. Sensitivity of the derived SAO pressure gradient conditions (unconstrained) using GFDL A2 and PCM A2 5

Table 2b. Sensitivity of the derived SAO pressure gradient conditions (unconstrained) using GFDL B1 and PCM B1 6

1.0 INTRODUCTION

California wildfire weather typically occurs during the fall season (September to December) prior to the winter rains, and when an inland high pressure and an offshore low pressure set up a strong pressure gradient with high offshore winds, heated air mass, and low humidity. These conditions are known locally as "Santa Ana winds" in southern California, and "Diablo winds" in northern California, and such conditions have a long history of being associated with the spread of wildfires. During Santa Ana and Diablo occurrences, hot downslope winds may exceed 60 miles per hours (mph), are warmed by adiabatic compression at a rate of 5°F per 1000 ft, and have a very low relative humidity, making these conditions the most prevalent for the spread of fires.

California fires linked to these hot and dry offshore flow conditions have resulted in significant loss of life and property, especially in regions where development has encroached on wilderness interfaces. In this initial study, Santa Ana conditions are analyzed using observations and simulated global climate model data for a historical period (1965–1994) and simulated climate data for projected periods (2005–2034, 2035–2064, 2070–2099). Our climate change fire weather sensitivity analyses are based on the output from two Atmosphere-Ocean General Circulation Models (AOGCMs): the NOAA GFDLv2 (Delworth et al., 2005) and the DOE/NCAR PCM (Washington et al. 2000), with simulations forced by the Intergovernmental Panel on Climate Change, Special Report on Emission Scenarios (IPCC SRES) high (A2) and low (B1) emissions scenarios (Nakićenović et al. 2000). These scenarios represent the range of IPCC non-intervention emissions futures with atmospheric CO_2 concentrations reaching approximately 550 parts per million (ppm) (B1) to 830 ppm (A2) by 2100.

2.0 APPROACH

Coastal California offshore flow is governed by several mechanisms, including the local sea breeze due to a diurnal land-sea temperature differential, and large scale atmospheric and ocean dynamics associated with pressure systems. It is largely thought that large-scale mechanisms dominate the Santa Ana and Diablo conditions, which are in turn modulated by local effects of the sea breeze and topography.

An approach for detecting Santa Ana Occurrences (SAOs) within AOGCM output has been developed here for the analysis of fire weather sensitivity due to climate change. The surface pressure and specific humidity fields were used as the available variables to determine the presence of SAOs. If available, the 850 hectopascal (hPA) geopotential height fields would also be used to further constrain the solution space. The weather conditions required for establishment of an SAO are the existence of a stationary high situated over the Great Basin and/or extending further east, an offshore Pacific low southwest of Los Angeles with a pressure difference between these centers of approximately 20 hPa, and the local (fire risk area) surface level humidity below approximately 40%. A search domain (125W 33N x 113W 39N) was used to define the region of expected high- and low-pressure fields that would result in the SAO northeasterly fire weather wind condition. The detection of SAOs depends on data availability, especially historical observations of changes in local wind and humidity. Station data representing local temperature, wind, and humidity were obtained from

Raphael (2003) for 1965 to 1994 and used as part of the bias evaluation along with the ERA40 Reanalysis (http://www.ecmwf.int/products/data/).

3.0 RESULTS

The initial SAO analysis is based on the hourly wind and humidity NCDC Surface Airways Observations (DS-3280) for California, Arizona, and the Western United States, and the ERA40 Reanalysis 850 hPa geopotential height, surface pressure, and specific humidity fields. A number of high SAO cases were identified and the search domain was configured. A very strong high offshore SAO-related fire occurred during December 1999, where fires spread and property loss was extensive. Figure 1 shows a four-day (19–22 December 1999, 20 December not shown) snapshot of the time evolving SAO using the available ERA40 geopotential height gradient, constrained by ERA40 specific humidity, indicting the large-scale Santa Ana fire weather conditions have set up. A parallel analysis (not shown) using surface pressure fields gave near identical patterns.

A 30-year (1965–1994) bias analysis was performed for the GFDL output, resulting in a good fit between the humidity-constrained, pressure-gradient-derived SAO days to the observed number of high offshore-wind, low-humidity SAO days. Figure 2 indicates that climatological (30-year average) September, October, November, and December, GFDL-simulated SAO days were 1.2, 3.5, 6.5, and 7.1 respectively, representing 109%, 78%, 94%, and 81% of observations, respectively. It is important to note that the seasonal trends match well, with September having the lowest number of SAO days and a near linear increase toward the maximum in December, with a near-linear decrease for the period during January and February (not shown). The slope of the September-to-December linear fit SAO days based on observations is 1.87 days/month and the GFDL-derived slope is 2.21 days/month.

This study analyzed the GFDL pressure gradients with and without humidity constraints for 1965–1994 and found that the humidity reduces the number of fall-season SAOs detected to 53% of those detected without humidity constraints. However, relative sensitivities are all consistent for both the constrained and unconstrained cases (Table 1), suggesting that the approach is valid and will provide new information on projected fire weather sensitivity under future climates.

SAO sensitivity (projected/historic) results for the three projected time periods (2005–2034, 2035–2064, 2070–2099) are presented in figures 3 and 4. Figure 3a was calculated with the inclusion of the available surface humidity as a constraint to the GFDL pressure gradient both for the projected and historical periods, but Figure 3b did not include humidity constraints for historical or projected periods. It is important to note that the mean-seasonal ratio between the constrained and unconstrained number of SAO days for all cases, including 1965–1994, is 49% (Table 1), verifying that for projected periods the constrained case remains about half the value of the unconstrained case. This is an important result, as this indicates there is a *consistent and relative* over-estimation for the unconstrained analyses, as compared to constrained. There is insufficient AOGCM output data (i.e., specific humidity, geopotential heights) at the time of this study to

impose a bias correction, hence this study evaluates the results as *relative sensitivities about the unconstrained simulations*, and this is discussed further in the summary.

The unconstrained GFDL-derived and PCM-derived SAOs for each month are summarized in Table 2a (A2) and 2b (B1). The relative SAO sensitivities range from 26% of historical (GFDL/A2 2070-2099 September) to 138% (PCM/A2 2070-2099 November). GFDL A2 and B1 outcomes indicate that the warmest fall season month, September, has an increase in SAO days in the early part of this century (120% of historical for both A2 and B1 during 2005-20035), followed by a decrease (26% for A2 and 88% for B1 during 2070–2099), while the PCM A2 and B1 outcomes suggest decreases in SAO during September (82% historical for A2 and 61% for B1 during 2005–2034; 45% historical for A2 and 82% for B1 during 2070–2099). Meanwhile, the strongest historical SAO month, December, decreases for all cases during the period 2005–2034 (GFDL/A2 89%, GFDL/B1 74%, PCM/A2 83%, PCM/B1 100.1%), and increases for the period 2070–2099 (GFDL/A2 110%, GFDL/B1 110%, PCM/A2 100.3%, PCM/B1 102.3%).

These initial findings indicate striking differences between early century and late century, and high-emission and lower-emission SAO sensitivities. The PCM results suggest an increase during October and November, with the greatest October increase (120%) during the 2005-2034 period with A2 emissions, and the greatest a November increase (125%–135%) at 2070–2099 for both A2 and B1. PCM additionally shows significant decreases for September and slight decreases for December. The GFDL SAO sensitivities are very different, with early century increases (125%) in SAO during September with a steady decrease toward the end of the century. October has increases in SAO for the B1 emissions and decreases for the A2 for all projected periods. November A2 is below the historical SAO for all periods, while the B1 emissions SAO results are at 100% during 2005–20034, 90% during 2035–2064, and 110% during 2070–2099. Finally, there are increased SAO for December at the end of the century, with below historical values for early and mid-century periods.

In terms of fire weather threats in the future, this initial study suggests that there may be SAO increases during critical dry periods, leading to more extensive wildfire. However, caution needs to be used with regard to these early results.

4.0 SUMMARY AND CONCLUSION

An initial analysis of pressure gradient-derived Santa Ana Occurrences has been described. Results suggest that during the fall season, SAOs may increase for some scenarios, while it may decrease for others. More research is required to fully establish the sensitivity of this mechanism under green house gas forcing.

The mean-annual and five-year running mean sea surface temperature (SST) and the number of SAO days is shown in Figure 5. It is interesting to note that there is a significant shift in the relationship between these two variables right at the 1976 Pacific multi-Decadal Oscillation (PDO) shift. This suggests that the role of natural variability in ocean temperatures, along with climate change SST variations, will play a significant role in the increase or decrease of the number of SAO days detected. Further analyses of climate types (positive El Niño Southern Oscillation (ENSO)/positive PDO; negative ENSO/positive PDO; positive ENSO/ negative PDO; negative ENSO/negative PDO), as

well as other natural climate modes will need to be decomposed to fully understand the sensitivity of SAOs.

This initial study begins to investigate an important climate impact on society, ecology and economy. This study only indicated the relative change in the number of SAO days and did not analyze the change in intensity and duration in consecutive SAO days. The missing aspects of this study are proposed as phase two, and will include more AOGCM output fields.

5.0 REFERENCES

Delworth, T. L., A. J. Broccoli, A. Rosati, R. J. Stouffer, et al. 2005. GFDL's CM2 global coupled climate models – Part 1 – Formulation and simulation characteristics. *J. Climate*, in press.

ERA40 http://www.ecmwf.int/products/data/archive/descriptions/e4/

Nakicenovic´, N., J. Alcamo, G. Davis, B. de Vries, J. Fenhann, S. Gaffin, K. Gregory, A. Grubler, T. Y. Jung, T. Kram, et al. 2000. Intergovernmental Panel on Climate Change Special Report on Emissions Scenarios. Cambridge Univ. Press, Cambridge, U.K.

Raphael, M. N. 2003. The Santa Ana winds of California. *Earth Interactions* **7,** 1-13.

Washington, W. M., J. W. Weatherly, G. A Meehl, A. J. Semtner, T. W. Bettge, A. P. Craig, W. G. Strand, J. Arblaster, V. B. Wayland, R. James, and Y. Zhang. 2000. *Clim. Dyn.* 16: 755–774.

Table 1. Evaluation of the derived SAO using GFDL A2 constrained and unconstrained by humidity

Evaluation	Season-Mean
GFDL (1965-1994) constrained/unconstrained	0.534433
GFDL (2005-2034) Constrained/unconstrained	0.449637
GFDL (2035-2064) constrained/unconstrained	0.496575
GFDL (2070-2099) constrained/unconstrained	0.479903

Table 2a. Sensitivity of the derived SAO pressure gradient conditions (unconstrained) using GFDL A2 and PCM A2

A2 Sensitivity	September	October	November	December	Season-Mean
GFDL (2005-2034)	1.224299	0.867742	0.941358	0.889655	0.934045
GFDL (2035-2064)	0.551402	0.787097	0.901235	0.968966	0.849661
GFDL (2070-2099)	0.261682	0.696774	0.79321	1.103448	0.796314
PCM (2005-2034)	0.818713	1.205056	1.198276	0.830769	1.035573
PCM (2035-2064)	0.690058	1.089888	1.172414	0.902564	1.000791
PCM (2070-2099)	0.450292	1.174157	1.37931	1.002564	1.079842

Table 2b. Sensitivity of the derived SAO pressure gradient conditions (unconstrained) using GFDL B1 and PCM B1

B1 Sensitivity	September	October	November	December	Season-Mean
GFDL (2005-2034)	1.233645	1.122581	1.098765	0.741379	1.019399
GFDL (2035-2064)	0.953271	1.032258	0.898148	0.910345	0.947624
GFDL (2070-2099)	0.88785	1.067742	1.015432	1.103448	1.042677
PCM (2005-2034)	0.614035	1.005618	0.994253	1.012821	0.951779
PCM (2035-2064)	0.590643	1.13764	1.178161	0.982051	1.026877
PCM (2070-2099)	0.824561	1.168539	1.267241	1.023077	1.104348

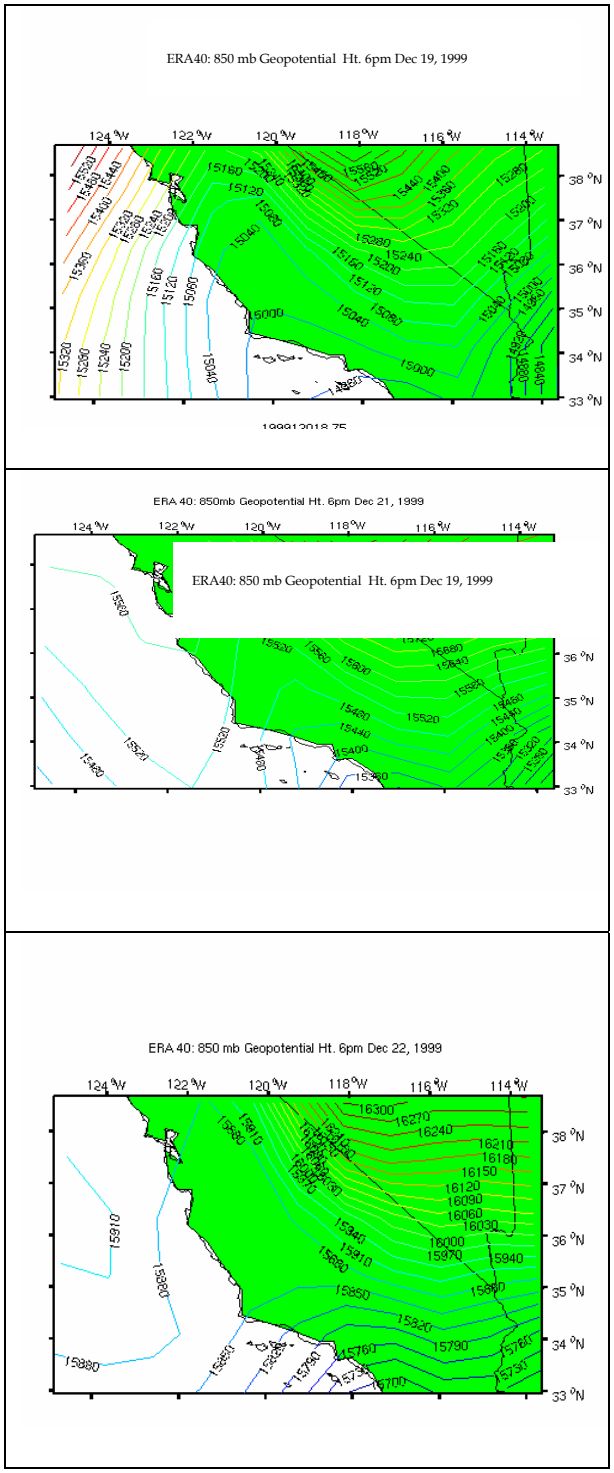

Figure 1. A four-day snapshot of the time evolving geopotential height fields, constrained by ERA40 specific humidity, associated with the December 1999 Santa Ana fires

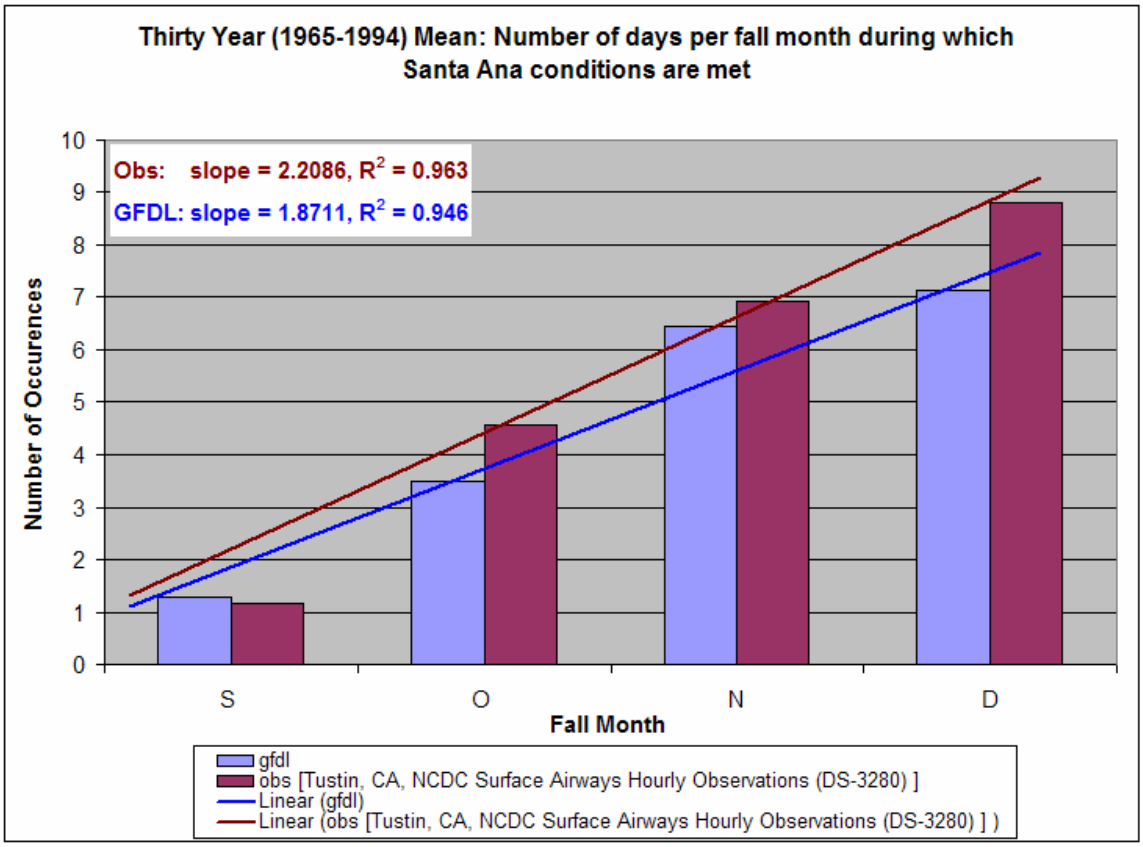

Figure 2. GFDL AOGCM-derived number of SAO days, based on the pressure gradient and humidity indicate a small bias for the monthly climatological occurrences

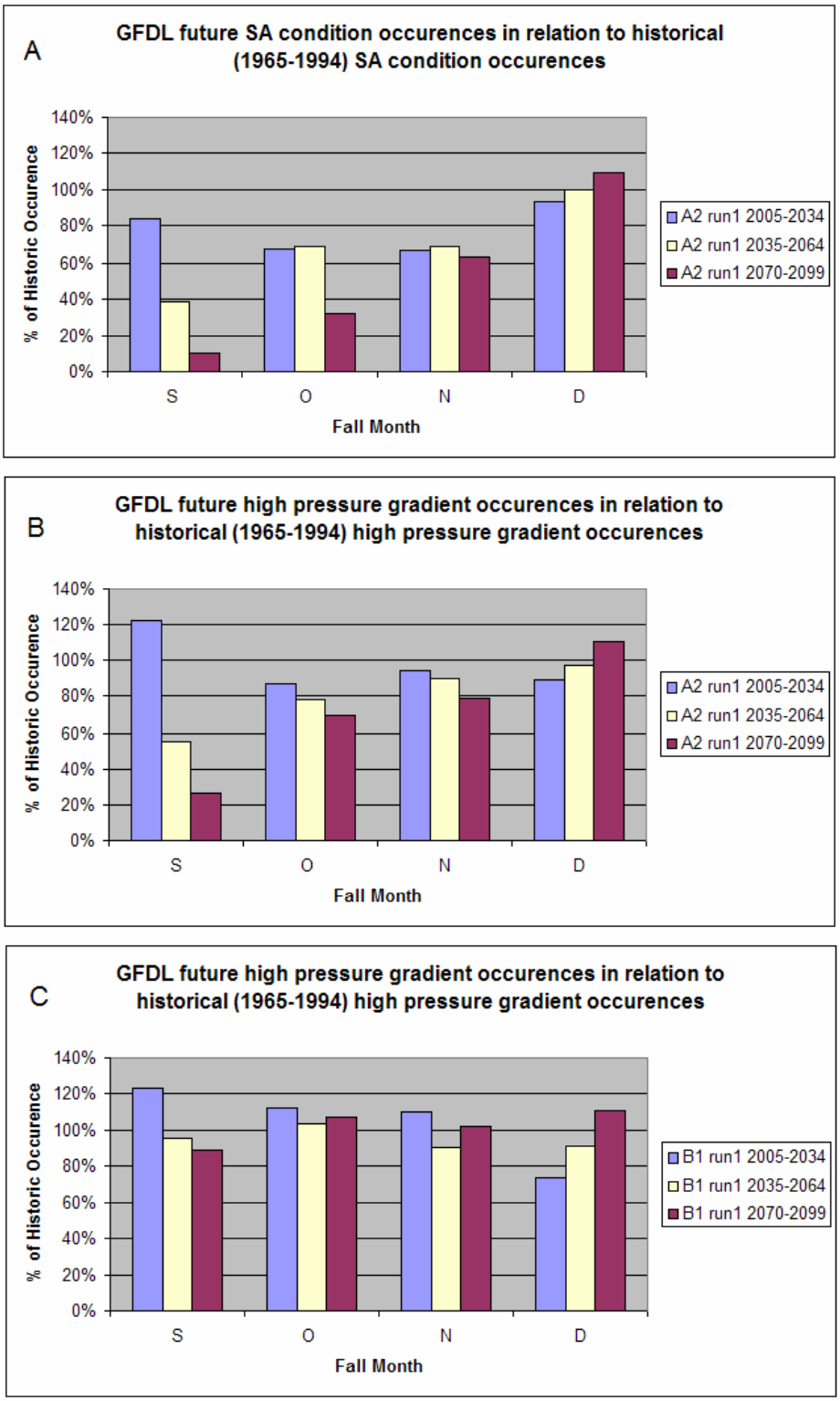

Figure 3. AOGCM-derived SAO sensitivity for 2005–2034, 2035–2064, and 2070–2099, based (A) GFDL pressure gradients and humidity with A2 forcing, (B) GFDL pressure gradients with A2 forcing, and (C) GFDL pressure gradients B1 forcing

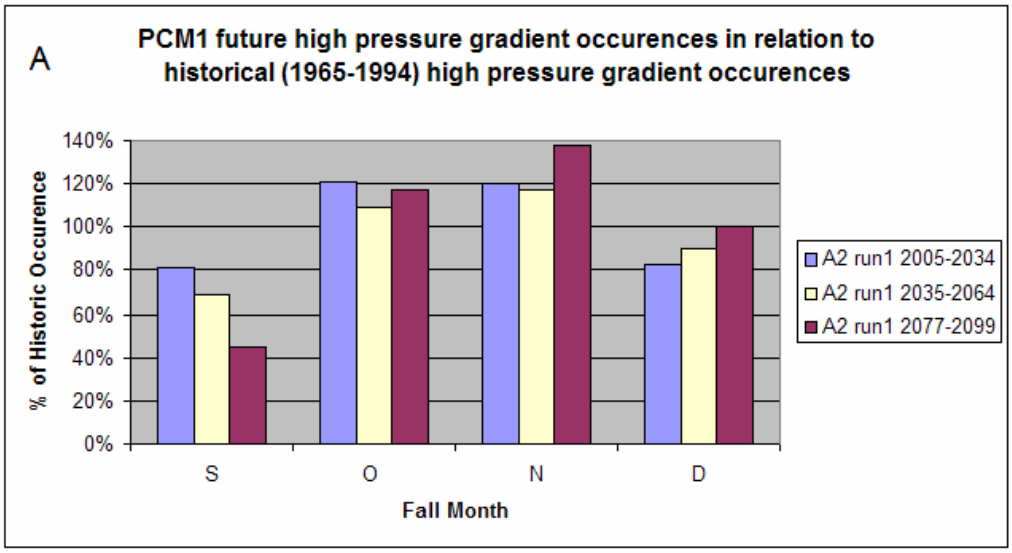

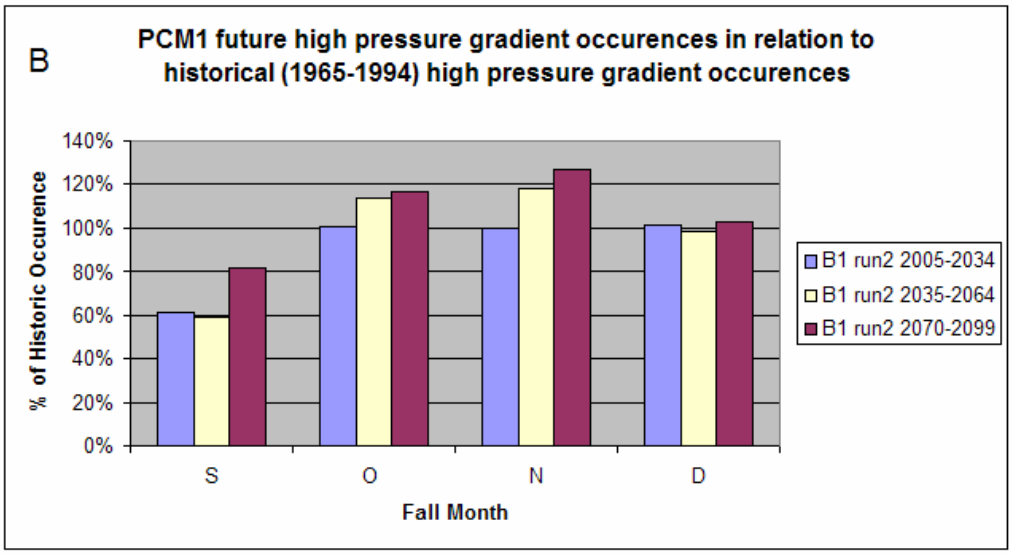

Figure 4. AOGCM-derived SAO sensitivity for 2005–2034, 2035–2064, and 2070–2099, based (A) PCM pressure gradients with A2 forcing, (B) PCM pressure gradients B1 forcing

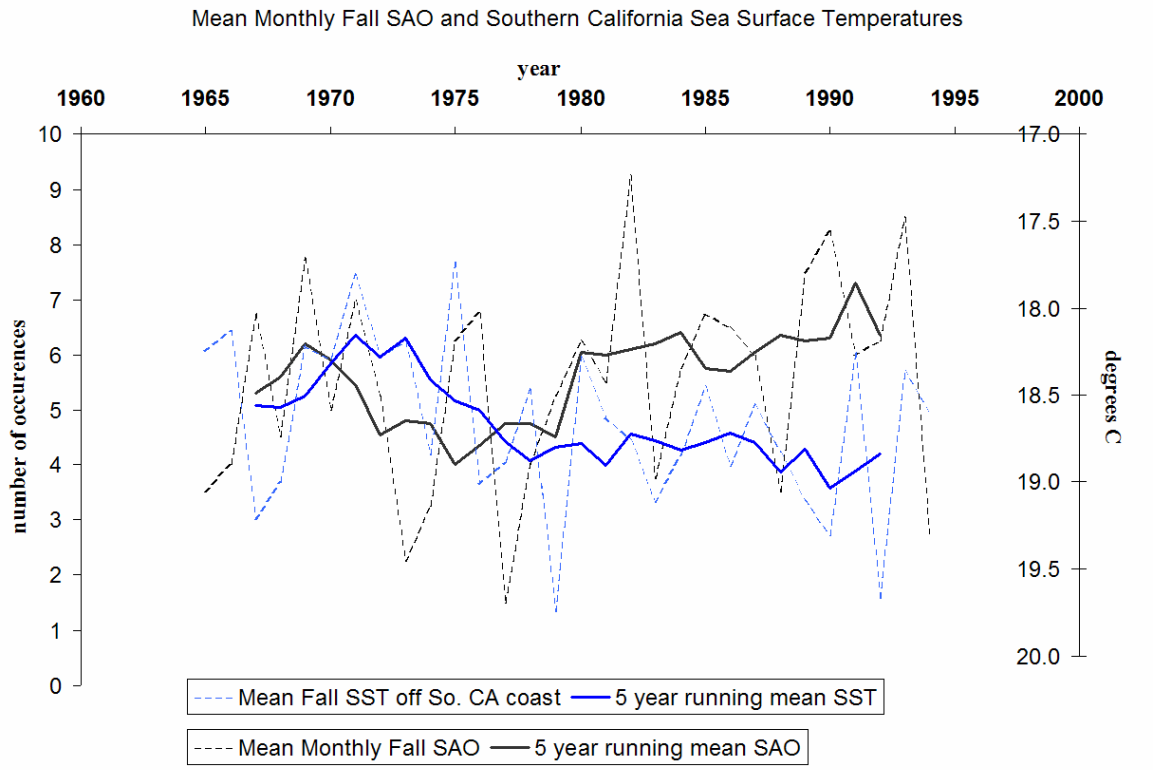

Figure 5. Comparison of the observed SAOs and southern California sea surface temperatures for September–December during 1965–1994